AtCAP2 is crucial for lytic vacuole biogenesis during germination by positively regulating vacuolar protein trafficking

Yun Kwon[a], Jinbo Shen[b], Myoung Hui Lee[c], Kyoung Rok Geem[a], Liwen Jiang[b,d], and Inhwan Hwang[a,c,1]

[a]Department of Life Sciences, Pohang University of Science and Technology, 37673 Pohang, Korea; [b]State Key Laboratory of Agrobiotechnology, Centre for Cell and Developmental Biology, School of Life Sciences, The Chinese University of Hong Kong, Shatin, New Territories, Hong Kong, China; [c]Division of Integrative Biosciences and Biotechnology, Pohang University of Science and Technology, 37673 Pohang, Korea; and [d]CUHK Shenzhen Research Institute, The Chinese University of Hong Kong, 518057 Shenzhen, China

Edited by Natasha V. Raikhel, Center for Plant Cell Biology, Riverside, CA, and approved December 29, 2017 (received for review October 9, 2017)

Protein trafficking is a fundamental mechanism of subcellular organization and contributes to organellar biogenesis. AtCAP2 is an *Arabidopsis* homolog of the *Mesembryanthemum crystallinum* calcium-dependent protein kinase 1 adaptor protein 2 (McCAP2), a member of the syntaxin superfamily. Here, we show that AtCAP2 plays an important role in the conversion to the lytic vacuole (LV) during early plant development. The *AtCAP2* loss-of-function mutant *atcap2-1* displayed delays in protein storage vacuole (PSV) protein degradation, PSV fusion, LV acidification, and biosynthesis of several vacuolar proteins during germination. At the mature stage, *atcap2-1* plants accumulated vacuolar proteins in the prevacuolar compartment (PVC) instead of the LV. In wild-type plants, AtCAP2 localizes to the PVC as a peripheral membrane protein and in the PVC compartment recruits glyceraldehyde-3-phosphate dehydrogenase C2 (GAPC2) to the PVC. We propose that AtCAP2 contributes to LV biogenesis during early plant development by supporting the trafficking of specific proteins involved in the PSV-to-LV transition and LV acidification during early stages of plant development.

lytic vacuole transition | vacuolar pH | vacuolar trafficking | intracellular trafficking | GAPC2 trafficking

Plants have two different types of vacuoles, the central lytic vacuole (LV) and the protein storage vacuole (PSV) (1). In flowering plants, seed embryonic cells contain PSVs but not LVs (2). LVs develop during germination and early seedling development. It has been proposed that PSVs fuse with each other during germination to generate LVs (3). A large number of factors are likely involved in LV biogenesis during germination. These factors may be produced as inactive forms during embryogenesis and subsequently activated during germination, and/or they may be newly produced and transported to PSVs during germination. In addition, LV proteins are newly produced during early germination and targeted to the newly forming LV. Indeed, during early germination, the levels of TIP3;1, a PSV-type tonoplast intrinsic protein (TIP), decrease with time, and concomitantly the levels of TIP1;1, an LV-type TIP, gradually increase, suggesting that PSVs are gradually converted to LVs via PSV-LV hybrids (1).

In *Saccharomyces cerevisiae*, many *Vacuolar Protein Sorting* (*VPS*) and *Vacuolar Morphology* (*VAM*) mutants have been identified that show defects in protein trafficking to the vacuole and vacuolar morphology (4–6). The *Arabidopsis* genome contains most of the yeast *VPS* homologs (7), and these genes are involved in intracellular trafficking and vacuole biogenesis. *VCL* (*Vacuoleless*) is a functional ortholog of yeast *VPS16*, and *vcl* plants lack LVs (8). VPS16 is a subunit of the homotypic fusion and protein sorting (HOPS) complex. Other *vps* mutants also display a common phenotype such as altered vacuolar morphology. These combined results suggest that protein trafficking is crucial for vacuole biogenesis in plants, similar to yeast. Consistent with this hypothesis, other proteins involved in trafficking such as PAT2, VFD1, and AMSH3 also have critical roles in vacuole biogenesis (9–11).

Protein trafficking has a crucial role in germination. In *Arabidopsis*, underexpression of the vacuolar sorting receptor blocks seed germination (12). Vacuolar sorting receptors are involved in sorting lytic vacuolar cargoes and PSV proteins, and localize to the Golgi apparatus, trans-Golgi network (TGN), and prevacuolar compartment (PVC). PSV proteins include 12S globulin, 2S albumin, and other seed storage proteins, which are expressed at high levels and trafficked to the PSV during seed maturation. LVs in vegetative tissues contain proteins that have an N-terminal propeptide sequence (11, 13, 14). A recent study showed that adaptor protein complex-3 (AP-3) is necessary for LV transition and function. Mutations of genes encoding β- or δ-subunits of AP-3 caused delays in vacuole biogenesis and germination (9, 15).

Although the basic mechanisms of protein trafficking in plant cells have been extensively investigated, the regulation of trafficking pathways with respect to intrinsic and environmental conditions is not fully understood. Our work examined potential regulatory factors of trafficking pathways, and we focused on

Significance

Plant cells contain two types of vacuoles: the lytic vacuole (LV) and protein storage vacuole (PSV). During embryogenesis, the LV is degenerated and PSVs are produced. Thus, embryonic cells in seeds contain PSVs but not LVs. The situation is reversed during germination, and vegetative cells contain the LV. Recent studies showed that vacuolar trafficking is crucial for LV biogenesis during germination. We identified AtCAP2 as a crucial factor for the vacuole transition during germination. AtCAP2 functions as a positive regulator of the vacuolar trafficking via prevacuolar compartment recruitment of GAPC2, an isoform of glyceraldehyde 3-phosphate dehydrogenases (GAPDHs), well-known metabolic enzymes involved in energy production via glycolysis. Thus, our study provides a connection between vacuolar trafficking and energy metabolism.

Author contributions: Y.K., L.J., and I.H. designed research; Y.K., J.S., M.H.L., and K.R.G. performed research; Y.K., J.S., and I.H. analyzed data; and Y.K., L.J., and I.H. wrote the paper.

The authors declare no conflict of interest.

This article is a PNAS Direct Submission.

Data deposition: Sequence data from this article can be found in the Arabidopsis Genome Initiative or GenBank/EMBL databases under the following accession numbers: Arabidopsis CAP2 (AAV74245), AALP (AT5g60360), SYP41 (AT5g26980), SYP51 (AT1g16240), SYP61 (AT1g28490), AtRabF1 (AT3g54840), Kam1 (AT2g20370), AtRabF2a (AT5g45130), VTI11 (AT5g39510), GAPC2 (At1g13440), and Sporamin (AAB52548).

[1]To whom correspondence should be addressed. Email: ihhwang@postech.ac.kr.

This article contains supporting information online at www.pnas.org/lookup/suppl/doi:10.1073/pnas.1717204115/-/DCSupplemental.

McCAP2 because it appeared to link trafficking and signaling pathways. *Mesembryanthemum crystallinum* calcium-dependent protein kinase 1 adaptor protein 2 (McCAP2) contains a coiled-coil spectrin repeat domain and belongs to the syntaxin superfamily. Previously, this protein was identified as a binding protein of calcium-dependent protein kinase 1 (McCPK1) (16). McCAP2 colocalizes with McCPK1 on vesicular structures and AtVTI1b, an *Arabidopsis* v-SNARE [vesicle-soluble *N*-ethyl maleimide-sensitive factor (NSF) attachment protein (SNAP) receptor] that localizes to the TGN and PVC when heterologously expressed in *Arabidopsis*. Many of the syntaxin superfamily proteins such as SNAREs participate in protein trafficking. However, unlike SNAREs, McCAP2 does not contain the transmembrane domain. Thus, McCAP2 was proposed as an adaptor in McCPK1 trafficking between the plasma membrane and nucleus (16).

Here, we examined whether *Arabidopsis* CAP2 (AtCAP2), a homolog of McCAP2, functions as a protein trafficking regulator. We performed genetic and cell biological studies to investigate the physiological role of AtCAP2. *Arabidopsis* contains three closely related McCAP2 homologs. Of these, we focused on AtCAP2, which displayed the highest sequence homology with McCAP2. We show that AtCAP2 has an important role in vacuolar trafficking by recruiting glyceraldehyde-3-phosphate dehydrogenase C2 (GAPC2), a glyceraldehyde 3-phosphate dehydrogenase (GAPDH) isoform, to the PVC, where it participates in the PSV-to-LV conversion. We also show that AtCAP2 is involved in LV acidification during the early stage of plant development.

Results

AtCAP2 Plays a Role in LV Biogenesis During Germination. The *Arabidopsis* genome encodes three McCAP2 homologs; of these, AtCAP2 is the most closely related McCAP2 homolog (*SI Appendix*, Fig. S1*A*). We identified a mutant plant, *atcap2-1* (SALK_209627), that had a transfer DNA (T-DNA) insertion at the 5′ untranslated region (UTR), which was confirmed by genotyping using specific primers (*SI Appendix*, Fig. S1 *B* and *C*). This loss-of-function mutant lacked *AtCAP2* transcripts (*SI Appendix*, Fig. S1*D*).

To investigate the physiological role of AtCAP2, we examined the phenotypes of *atcap2-1* plants, and found that they did not display any noticeable morphological alterations. Then, we examined if these plants had any defects at the cellular level. During germination of wild-type seeds, one of the most prominent changes is the fusion of PSV to each other to give rise to the LV (17, 18). The *atcap2-1* mutant showed delayed germination compared with wild-type seeds (*SI Appendix*, Fig. S1*E*). At 48 h, germination of wild-type seeds was complete, whereas the germination rate of *atcap2-1* seeds was reduced to 60% (*SI Appendix*, Fig. S1*F*). The germination delay in *atcap2-1* seeds was rescued by expression of *AtCAP2:GFP*, confirming that the delay is caused by *AtCAP2* mutation. To test for any abnormalities in vacuole morphology during germination, we stained germinating seedlings with 2′,7′-bis(2-carboxyethyl)-5,6-carboxyfluorescein acetoxymethyl ester (BCECF-AM), which accumulates in the vacuole (17, 19, 20). At 3 d after germination (DAG), wild-type seedlings contained a large single LV in root tip and root epidermal cells, whereas *atcap2-1* seedlings displayed severely fragmented vacuoles (Fig. 1*A*). Expression of *AtCAP2:T7* in *atcap2-1* plants rescued the fragmented vacuole phenotype, confirming that vacuole fragmentation is caused by *AtCAP2* mutation. However, neither wild-type nor *atcap2-1* plants displayed any noticeable differences in PSV morphology during embryogenesis (Fig. 1*B*). These results indicate that the conversion of PSVs to the LV is delayed in *atcap2-1* plants.

In seed cells, PSVs have neutral pH. During germination, the vacuolar pH in PSVs becomes more acidic along with conversion of the PSV to the LV. Vacuole acidification is important for processing storage proteins in PSVs during germination because

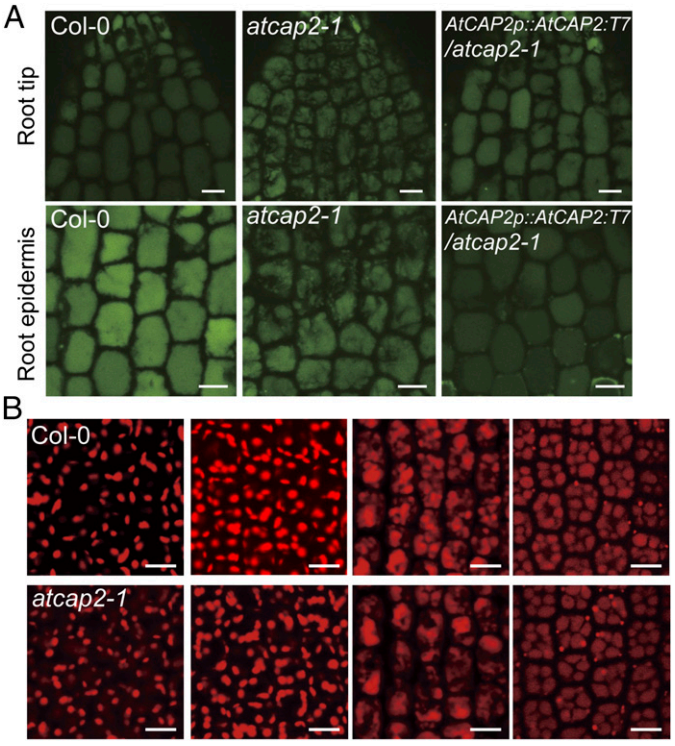

Fig. 1. Mutant *atcap2-1* plants display a delay in lytic vacuole biogenesis. (*A*) Morphology of LV during germination. *Arabidopsis* seeds were planted on 1/2 MS plates. At 3 d after planting, seeds with emerging radicles were dissected and stained with the vacuole-staining dye BCECF-AM for 1 h. Images of vacuoles in root cells in the division zone were captured with laser excitation at 488 nm. (*B*) Autofluorescence of protein storage vacuoles in developing and developed embryos in *Arabidopsis* seeds. Developing embryos were isolated from immature seeds of green siliques. (Scale bars: 10 μm.)

vacuolar proteolytic enzymes require an acidic environment (21). Thus, pH change can be a good indicator of PSV conversion to LV during germination (22). We measured the vacuolar pH of cells in the root division zone using the dual-excitation ratiometric pH indicator BCECF-AM (20) (Fig. 2*A*). BCECF-AM is uncharged and rapidly diffuses into cells. Once it enters into a cell, intracellular esterases hydrolyze its ester bond to release BCECF, a pH-dependent fluorophore. Intracellular pH can be measured by the pH-dependent ratio of the fluorescence emission intensities (detected at 550 nm) following BCECF excitation at 458 and 488 nm (23). First, we measured vacuole pH in radicle cells or root cells at 1–2 DAG. In wild-type plants, cells at 1–2 DAG contain 5–6 small vacuoles with a pH of 4.9 ± 0.06. In *atcap2-1* plants, the vacuolar pH was 5.28 ± 0.08 (*SI Appendix*, Fig. S2*A*), indicating that *atcap2-1* plants have higher vacuolar pH. At 3 DAG, the vacuolar pH ranged from 5.7 to 5.9 in wild-type seedlings, but was 6.0–6.3 in *atcap2-1* seedlings (Fig. 2*B*). These results indicate that *atcap2-1* seedlings have a defect in vacuole acidification.

Another important feature that accompanies PSV conversion to the LV is storage protein degradation (18, 24). When we examined the degradation of two storage proteins at the biochemical level (Fig. 2*C*), total proteins were extracted from embryos at different time points after germination, and then separated by SDS/PAGE. The levels of storage proteins such as 12S globulins gradually declined over time in wild-type seedlings. However, these storage proteins were degraded more slowly in *atcap2-1* seedlings. At 48 and 72 h after germination, 12S globulin levels in *atcap2-1* seedlings were 40%

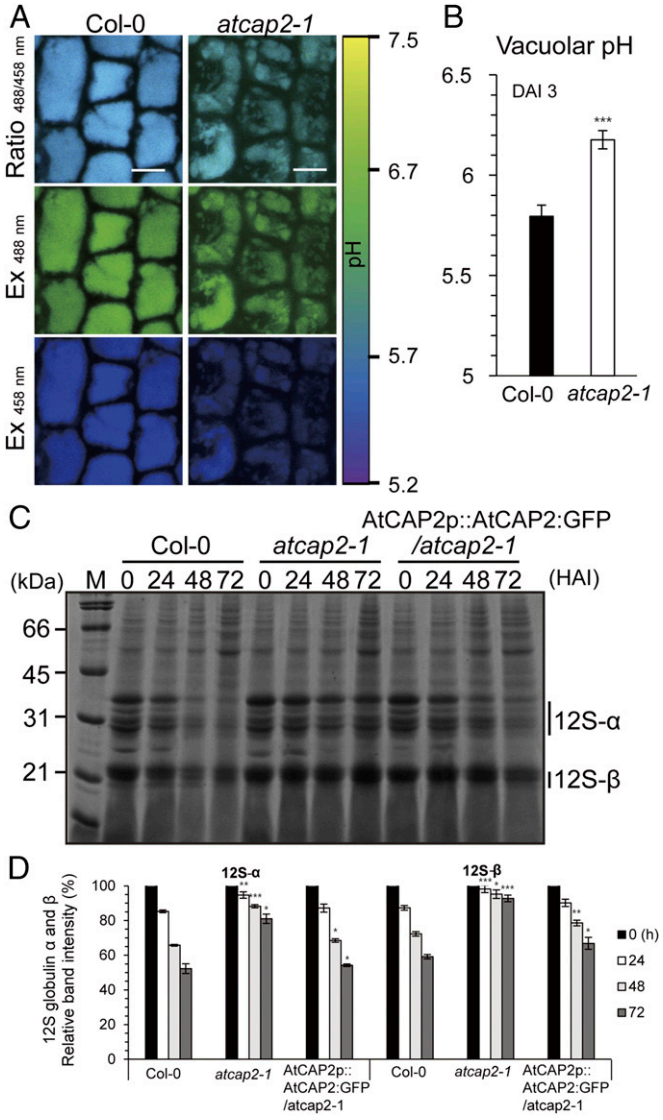

Fig. 2. Mutant *atcap2-1* plants display a defect in lytic vacuole acidification and storage protein degradation in the protein storage vacuole. (*A*) Images of the dye (BCECF-AM)-stained vacuoles. Wild-type and *atcap2-1* seedlings were germinated for 3 d and then stained with BCECF-AM for 1 h. Images of vacuoles in root tip cells were taken after laser excitation at 458 nm (*Bottom*) and 488 nm (*Middle*). The ratio images are shown in the *Top*. (Scale bars: 10 μm.) (*B*) Vacuolar pH. Images (*A*) were analyzed to measure the pH according to the basis of a calibration curve (*SI Appendix*, Fig. S3*C*). Statistical analysis was performed using Student's *t* test by comparing *atcap2-1* with Col-0. Asterisks indicate significant differences; $***P < 0.001$. Error bars show the SD ($n = 10$). (*C*) Delayed degradation of storage proteins in *atcap2-1* seedlings. Protein extracts were prepared at the indicated time points after germination and separated using 12% SDS/PAGE. Gels were stained with Coomassie Brilliant Blue R-250. 12S-α, 12S globulin α subunit; 12S-β, 12S globulin β subunit. (*D*) Quantification of 12S globulin degradation during germination. Band intensities of α and β subunits of 12S globulins at different time points in *C* were measured using dedicated LAS4000 software (FujiFilm Multi Gauge Version 2.2). The numbers represent values relative to the value at time 0. Statistical analysis was performed using Student's *t* test by comparing *atcap2-1* with Col-0 at the indicated time points. Asterisks indicate significant differences; $*P < 0.1$; $**P < 0.01$; $***P < 0.001$. Error bars, SD ($n = 3$).

and 20% higher, respectively, than those in wild-type seedlings (Fig. 2*D*). These results are consistent with the proposal that *atcap2-1* plants have a delay in the transition of the PSV to the LV.

Protein Trafficking to the Vacuole Is Delayed in *atcap2-1* Plants. Some mutant plants with defective protein trafficking also have a delay in LV biogenesis (11). To gain insight into the role of AtCAP2 in LV biogenesis, we tested for a defect in protein trafficking to the LV in *atcap2-1* plants. We generated transgenic plants harboring dexamethasone (Dex)-inducible chimeric vacuolar reporter protein constructs (*Spo:GFP* and *AALP:GFP*). The Spo:GFP construct contains the N-terminal domain of sweet potato sporamin fused to GFP; the AALP:GFP construct contains *Arabidopsis* aleurain-like protease (AALP) and GFP (14, 25–27). These transgenic plants were crossed with *atcap2-1* plants, and then homozygous plants for both *atcap2-1* and *Spo:GFP* or *atcap2-1* and *AALP:GFP* (Spo:GFP/*atcap2-1* and AALP:GFP/*atcap2-1* plants) were obtained from the F_2 generation.

First, we used confocal microscopy to examine the trafficking of Spo:GFP or AALP:GFP in *Spo:GFP*/*atcap2-1* or *AALP:GFP*/*atcap2-1* plants, respectively, to confirm whether the delay in vacuole biogenesis is caused by a defect in vacuolar trafficking. However, GFP fluorescence was below the detection limit due to low expression levels after Dex treatment during early germination. Then, we used 5-d-old seedlings and examined the trafficking of Spo:GFP and AALP:GFP. Protoplasts from wild-type or *atcap2-1* plants harboring Dex-inducible *Spo:GFP* were treated with 30 μM Dex, and Spo:GFP localization was examined 24 and 36 h after the start of incubation. The majority of wild-type protoplasts expressing *Spo:GFP* showed a vacuolar pattern. However, the majority of Spo:GFP/*atcap2-1* protoplasts showed either a large cellular network or punctate staining patterns (Fig. 3*A*). Similarly, AALP:GFP also localized to a large cellular network and/or punctate staining pattern in the *atcap2-1* background, instead of the vacuolar pattern observed in wild-type protoplasts. These results indicate that protein trafficking to the LV is significantly delayed in *atcap2-1* plants within 5 DAG. We quantified the trafficking efficiency of Spo:GFP and AALP:GFP. Protein extracts prepared at 24 and 36 h after Dex treatment were analyzed by Western blotting using anti-GFP antibody (26). The trafficking efficiency of Spo:GFP was reduced from 83% in wild-type protoplasts to 59% in *atcap2-1* protoplasts, whereas that of AALP:GFP was reduced from 90 to 69% (Fig. 3 *B* and *C*). To validate that the observed defect in vacuolar trafficking in *atcap2-1* plants was caused by the *AtCAP2* mutation, we generated transgenic plants harboring both *AtCAP2p::AtCAP2:T7* and Dex-inducible *Spo:GFP* or *AALP:GFP* in *atcap2-1* plants by introducing *AtCAP2* driven by its own promoter and tagged with T7 (*AtCAP2p::AtCAP2:T7*) into *Spo:GFP*/*atcap2-1* or *AALP:GFP*/*atcap2-1* plants. Protoplasts were prepared from 5-d-old seedlings of these transgenic plants and treated with Dex for 24 or 36 h, and then proteins were extracted and analyzed by Western blotting using anti-GFP and T7 antibodies. The trafficking efficiency of both Spo:GFP and AALP:GFP in these protoplasts harboring *AtCAP2p::AtCAP2:T7* was recovered to the levels in wild-type protoplasts (*SI Appendix*, Fig. S3), indicating that the delayed vacuolar trafficking of Spo:GFP and AALP:GFP in *atcap2-1* plants is caused by the mutation.

To identify the location of AALP:GFP and Spo:GFP accumulation in *atcap2-1* plants, we performed colocalization experiments with organellar marker proteins such as *mRFP:AtRabF2a*, *mRFP:SYP61*, or *KAM1(ΔC):mRFP*. We transformed *AALP:GFP* or *Spo:GFP* into *atcap2-1* protoplasts together with each of these organellar marker plasmids and examined the colocalization of AALP:GFP or Spo:GFP with the organellar markers. The majority of Spo:GFP (90.8%) and AALP:GFP (85.9%) colocalized with mRFP:AtRabF2a at the PVC (*SI Appendix*, Fig. S4), indicating that the *atcap2-1* mutation affects trafficking of Spo:GFP and AALP:GFP from the PVC to the LV.

Next, we examined the trafficking of membrane cargo to the tonoplast. AtβFruct4N is an N-terminal, 84-amino acid residue fragment of AtβFruct4, which is sufficient for tonoplast targeting as a GFP fusion protein (AtβFruct4N:GFP). When AtβFruct4N:GFP

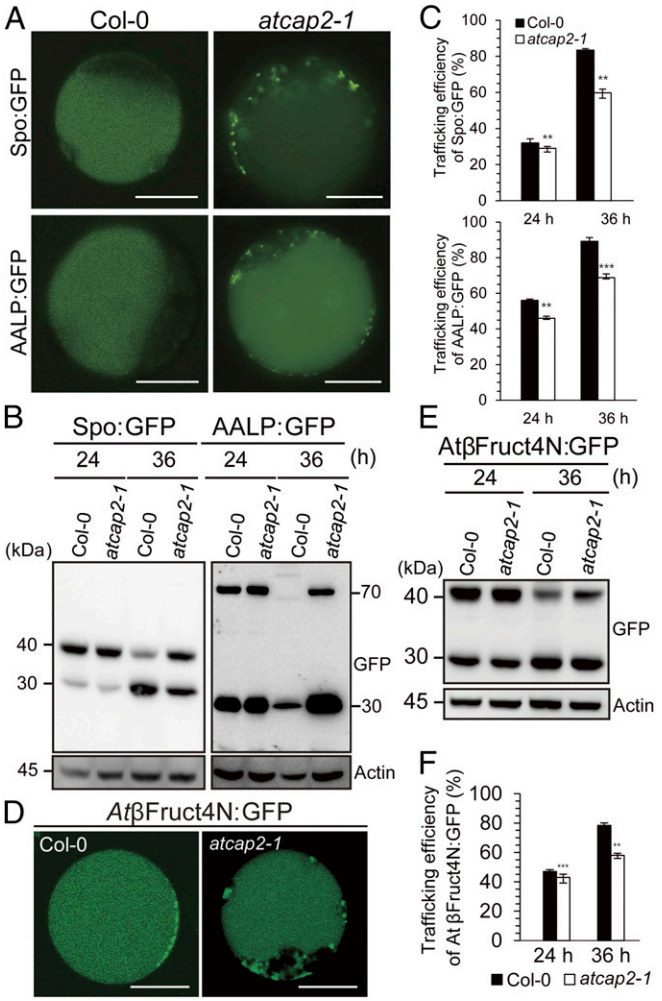

Fig. 3. Mutant *atcap2-1* plants display a defect in protein trafficking to the lytic vacuole. (*A*) Vacuolar trafficking of Spo:GFP and AALP:GFP in *atcap2-1* protoplasts. Protoplasts were isolated from *atcap2-1* mutant seedlings harboring Dex-inducible *Spo:GFP* or *AALP:GFP*. Protoplasts were treated with 30 μM Dex, and protein localization was examined 36 h after Dex treatment. (*B*) Western blot analysis of vacuolar trafficking of AALP:GFP and Spo:GFP. Protein extracts from protoplasts were analyzed by Western blotting using anti-GFP antibody. Actin was detected using anti-actin antibody to use as a loading control. (*C*) Quantification of trafficking efficiency. To quantify the trafficking efficiency, intensities of the bands in the immunoblot of Spo:GFP or AALP:GFP in *B* were measured using software equipped to LAS4000. The trafficking efficiency was calculated by dividing the processed forms with the total expressed proteins. Statistical analysis was performed using Student's *t* test by comparing *atcap2-1* with Col-0 at the indicated time points. Asterisks indicate significant differences; $^{**}P < 0.01$; $^{***}P < 0.001$. Error bars, SD ($n = 3$). (*D–F*) Trafficking of AtβFruct4N:GFP in *atcap2-1* plants. Protoplasts from WT and *atcap2-1* plants were transformed with *AtβFruct4N:GFP*. (*D*) The localization of AtβFruct4N:GFP was examined at 36 h after transformation. (*E*) Protein extracts from protoplasts were analyzed by Western blotting using anti-GFP antibody. (*F*) To quantify trafficking efficiency, signal intensities of the protein bands in the immunoblot in *E* were measured and represented as relative values. Statistical analysis was performed using Student's *t* test by comparing *atcap2-1* with Col-0 at the indicated time points. Asterisks indicate significant differences; $^{**}P < 0.01$; $^{***}P < 0.001$. Error bars, SD ($n = 3$). (Scale bars: 20 μm.)

is targeted to the tonoplast, GFP is cleaved from the fusion protein and released into the vacuole lumen, resulting in a luminal vacuolar pattern (26, 27). AtβFruct4N:GFP produced a punctate pattern together with the luminal vacuolar pattern in *atcap2-1* protoplasts, compared with wild-type protoplasts that displayed only the vacuolar luminal pattern (Fig. 3*D*), indicating a defect in AtβFruct4N:GFP vacuolar trafficking. The trafficking efficiency of AtβFruct4N:GFP was reduced from 78% in wild-type protoplasts to 58% in *atcap2-1* protoplasts (Fig. 3 *E* and *F*). These results indicate that AtCAP2 plays a role in the trafficking of several soluble and membrane proteins to the LV.

During germination, the newly forming LV needs a large amount of vacuolar proteins that are newly synthesized and transported through protein trafficking. To further examine the contribution of AtCAP2 to LV biogenesis, we examined the profiles of the endogenous proteins AALP and TIP1;1 (γ-TIP) in seedlings of germinating seeds by performing Western blot analysis with anti-AALP and anti-TIP1;1 antibodies, respectively. TIP1;1 (γ-TIP) is an aquaporin that specifically localizes to the LV tonoplast (28). During germination, the levels of AALP and TIP1;1 increased in both wild-type and *atcap2-1* plants in a time-dependent manner. However, the levels were significantly lower in *atcap2-1* seedlings than in wild-type seedlings at the same time points, indicating that *atcap2-1* seedlings have a defect in the accumulation of lytic vacuolar proteins (Fig. 4). To exclude the possibility that the mutation causes overall inhibition of the gene expression, we examined other proteins as control. The levels of PIP2;1, BiP, and α-tubulin were essentially the same in *atcap2-1* and in wild-type seedlings, indicating that the defect in organellar protein accumulation is specific to lytic vacuolar proteins. To confirm that the phenotype is resulted by atcap2 mutations, we performed the same experiments with complemented plants (AtCAP2p::AtCAP2:T7) and found that the vacuolar protein levels in complemented plants were recovered to the levels in wild-type plants. These results are consistent with the results showing that *atcap2-1* plants have a defect in protein trafficking to the LV.

We examined the specificity of AtCAP2 in protein trafficking. Invertase:GFP, a chimeric protein containing secretory invertase and GFP (29), was efficiently secreted in both wild-type and *atcap2-1* protoplasts (*SI Appendix*, Fig. S6*A*). Similarly, H^+-ATPase:RFP, a chimeric protein containing plasma membrane H^+-ATPase and RFP, was properly targeted to the plasma membrane (*SI Appendix*, Fig. S6*B*). These combined results

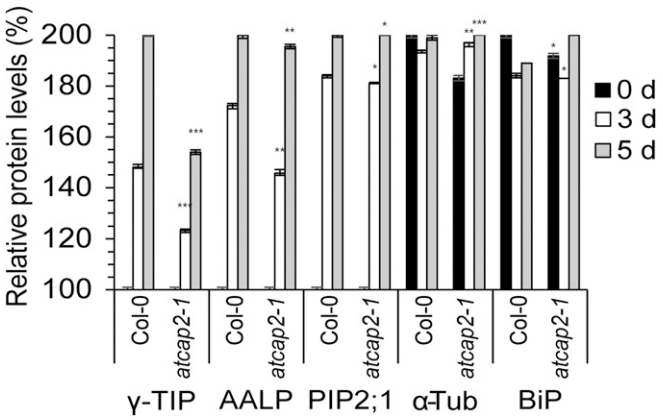

Fig. 4. Mutant *atcap2-1* plants have defective biogenesis of nascent lytic vacuolar proteins during early germination. Protein profiles in germinating *Arabidopsis* seeds. Total proteins were obtained from germinating seeds at the indicated time points from day 0 to day 5 after germination (0–5 DAG) and analyzed by Western blotting using various antibodies as indicated. To quantify protein levels, the intensities of protein bands in *SI Appendix*, Fig. S5 were measured and represented as relative protein values with respect to that of the 0 time point, which was set to 100%. Three independent experiments were performed. Error bars show SE ($n = 3$). α-Tub, α-tubulin; BiP, endoplasmic reticulum binding protein; γ-TIP, tonoplast intrinsic protein; PIP2;1, plasma membrane intrinsic protein.

indicate that AtCAP2 is not involved in the trafficking of secretory or plasma membrane proteins.

AtCAP2 Localizes to the PVC as a Peripheral Membrane Protein. To corroborate the role of AtCAP2 in vacuolar trafficking, we examined its subcellular localization. McCAP2 localizes to the PVC (16). Protoplasts from leaf tissues were transformed with *AtCAP2:mRFP*, and the resulting localization pattern was examined in more than 50 protoplasts. AtCAP2:mRFP produced a punctate staining pattern in addition to diffuse cytosolic signals. To define the organelle to which AtCAP2:mRFP localizes, AtCAP2:mRFP was cotransformed with several organellar marker constructs. Sialyltransferase (ST):GFP localizes to the Golgi apparatus; GFP:SYP41 (30), GFP:SYP61, and AtRabF1:GFP localize at the TGN (31, 32); and GFP:SYP51 (31, 33), GFP:AtRabF2a (34), and VTI11:GFP (34, 35) localize to the PVC. Among these markers, the punctate staining patterns of AtCAP2:mRFP merged with those of GFP:SYP51, GFP:AtRabF2a, and VTI11:GFP, but not with those of ST:GFP (Fig. 5*A*), GFP:SYP41, GFP:SYP61, and AtRabF1:GFP (*SI Appendix*, Fig. S7). These results indicate that AtCAP2:mRFP largely localizes to the PVC. Thus, AtCAP2 localization is consistent with that of McCAP2 (16).

Protein sequence analysis showed that AtCAP2 does not contain any transmembrane domains. To test whether AtCAP2 is a peripheral membrane protein, protein extracts from AtCAP2:GFP transgenic plants were separated into soluble and membrane fractions by ultracentrifugation, and then analyzed by Western blotting using anti-GFP antibody. AtCAP2:GFP was present in both soluble and membrane fractions. AtCAP2:GFP in the membrane fraction was solubilized by sodium bicarbonate (0.1 M, pH 11.1), indicating that it associates with membranes via ionic interactions (Fig. 5*B*). These results suggest that AtCAP2 is peripherally localized at the PVC in addition to the large proportion in the cytosol as a soluble form.

AtCAP2 Interacts with GAPC2 Localized to the PVC. To further elucidate the underlying mechanism by which AtCAP2 plays a role in vacuolar trafficking, we identified its interacting proteins. We performed coimmunoprecipitation (co-IP) experiments with protein extracts of AtCAP2:GFP plants using anti-GFP antibody followed by LC-MS/MS spectrometry and MALDI-TOF analysis. As a negative control, we used plants harboring GFP alone (*SI Appendix*, Fig. S8). Proteins identified from LC-MS/MS analysis included GAPC2, an isoform of GAPDHs. GAPCs were detected in vesicle-associated protein fractions, and were shown to be involved in protein trafficking (36–39) and membrane fusion in animal and plant cells (40–42). GAPCs also activate PLDδ, which is responsible for phosphatidic acid (PA) production and interacts with PA (43). PA plays a critical role in vesicle formation (44). We confirmed the interaction of AtCAP2 with GAPC2 by co-IP experiments using anti-GAPC2 antibody. The specificity of anti-GAPC2 antibody was examined using protein extracts of wild-type and *gapc2* plants (*SI Appendix*, Fig. S9*B*). The *gapc2* plants had a T-DNA insertion at *GAPC2*. Protein extracts from plants expressing AtCAP2:GFP were subjected to reciprocal co-IP experiments using anti-GFP or anti-GAPC2 antibodies, and the immunoprecipitates were analyzed by Western blotting using anti-GAPC2 or anti-GFP antibodies. The reciprocal co-IP experiments showed that AtCAP2 (60 kDa) interacts with GAPC2 (43 kDa) (Fig. 6 *A* and *B*). These results support the proposal that AtCAP2 and GAPC2 are involved in vacuolar trafficking and conversion of the PSV to the LV during germination.

To obtain supporting evidence that GAPC2 functions together with AtCAP2 in vacuolar trafficking during early germination, we examined whether *GAPC2* and *AtCAP2* are expressed during germination. For *GAPC2*, we prepared protein extracts from germinating seeds and 5-d-old seedlings of wild-type and *gapc2* plants, and performed Western blot analysis using anti-GAPC2

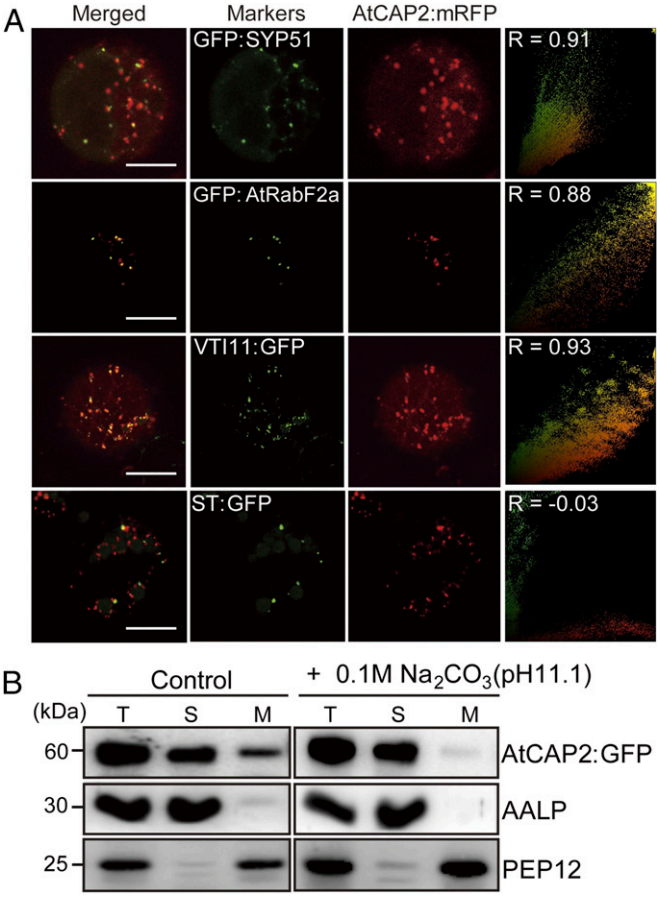

Fig. 5. AtCAP2:mRFP primarily localizes to the prevacuolar compartment. (*A*) *AtCAP2:mRFP* was transformed into wild-type protoplasts together with the indicated organellar marker constructs, *GFP:SYP51*, *GFP:AtRabF2a*, *VTI11:GFP*, and *ST:GFP*. The localization was examined at 36 h after transformation. To quantify the degrees of colocalization between AtCAP2:mRFP and organellar markers, images of more than 50 cells were analyzed using ImageJ 1.51J8 (National Institutes of Health), and the results are presented as scatter plots with Pearson's coefficients. (Scale bars: 20 μm.) (*B*) Subcellular fractionation of AtCAP2:GFP. Protein extracts from transgenic plants expressing *AtCAP2:GFP* were centrifuged at 10,000 × *g* for 10 min, and the supernatants were further separated into soluble and pellet fractions by ultracentrifugation at 100,000 × *g* for 90 min. The pellet fractions were further treated with 100 mM Na_2CO_3, pH 11.1, and then subjected to ultracentrifugation again to separate soluble and membrane fractions. Supernatant and pellet fractions were separately collected and used for Western blot analysis using anti-GFP body. Anti-AALP and anti-PEP12 antibodies were used to detect endogenous AALP and PEP12 as representatives of soluble and integral membrane proteins, respectively. M, pellet fraction; S, supernatant; T, total protein extracts.

antibody (*SI Appendix*, Fig. S9*A*). The results showed that GAPC2 was expressed in germinating seeds and young seedlings. For *AtCAP2*, we examined RNA transcript expression levels in wild-type and *atcap2-1* seeds using *AtCAP2*-specific primers because we did not have an AtCAP2 antibody. The results showed that *AtCAP2* transcripts were strongly detected in wild-type seeds but not in *atcap2-1* seeds (*SI Appendix*, Fig. S9*B*). To support these RT-PCR results, we examined AtCAP2:T7 levels in transgenic plants harboring *AtCAP2p::AtCAP2:T7* using anti-T7 antibody. AtCAP2:T7 was expressed in both seeds and 5-d-old seedlings (*SI Appendix*, Fig. S9*C*).

To elucidate the precise relationship between AtCAP2 and GAPC2 in trafficking, we postulated that AtCAP2 may function as an adaptor for the localization of GAPC2 to the PVC. Previously,

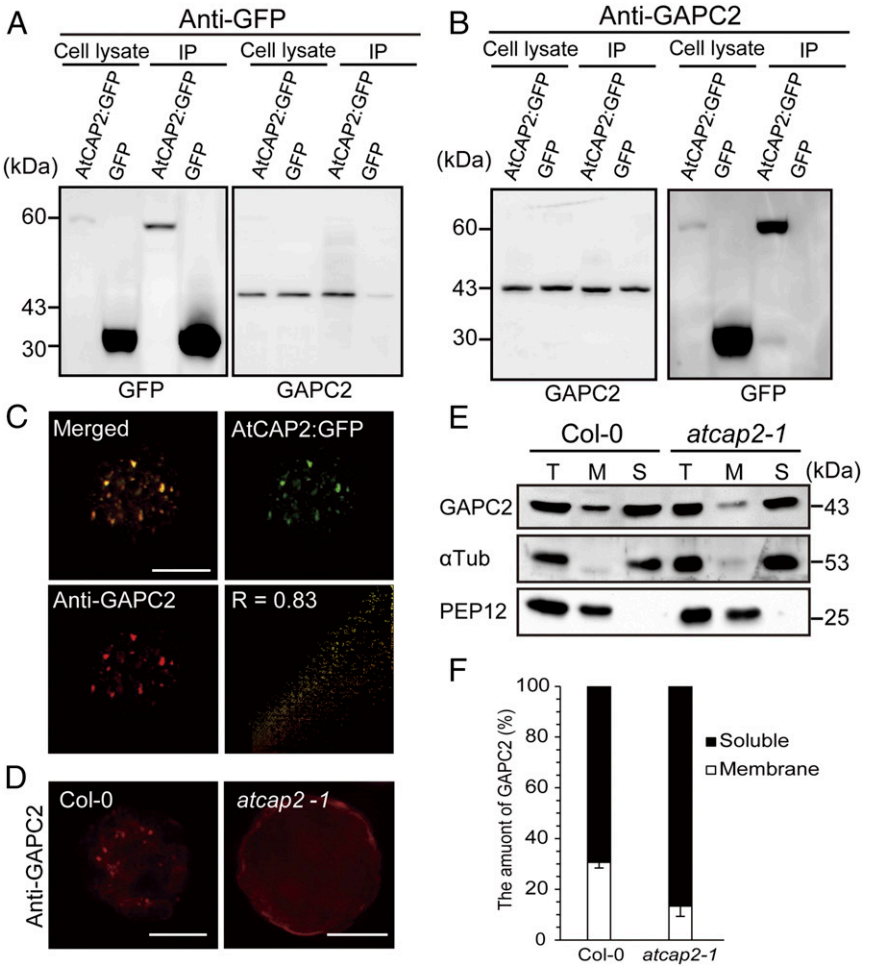

Fig. 6. GAPC2 interacts with AtCAP2 and localizes to the PVC. (*A* and *B*) Coimmunoprecipitation of AtCAP2:GFP with GAPC2. Protein extracts from transgenic plants harboring *AtCAP2:GFP* or *GFP* alone were subjected to immunoprecipitation with anti-GFP (*A*) or anti-GAPC2 (*B*) antibodies, and the immunoprecipitates were analyzed by Western blotting using anti-GAPC2 or anti-GFP antibodies as indicated. (*C*) Localization of GAPC2. Protoplasts from transgenic plants expressing *AtCAP2:GFP* were immunostained with anti-GAPC2 antibody as the primary antibody followed by staining with TRITC-labeled anti-rabbit IgG as the secondary antibody. GFP signals of AtCAP2:GFP were directly observed. The images obtained from more than 50 protoplasts were analyzed using ImageJ 1.51J8 (National Institutes of Health), and the results were presented as a scatter plot with Pearson's coefficient. (*D*) Failure of GAPC2 subcellular localization to the PVC in *atcap2-1* plants. Protoplasts from wild-type and *atcap2-1* plants were immunostained with anti-GAPC2 antibody, followed by staining with a secondary anti-rabbit IgG labeled with TRITC. Images were acquired by a laser scanning confocal microscope (LSM510; Carl Zeiss). (*E*) Subcellular fractionation of GAPC2 in *atcap2-1* plants. Total extracts from wild-type and *atcap2-1* plants were separated into soluble and pellet fractions by ultracentrifugation at 100,000 × *g* for 90 min. The supernatant and membrane fractions were analyzed by the Western blotting using various antibodies as indicated. Anti-GAPC2, anti-AALP, and anti-PEP12 antibodies. Anti-AALP and anti-PEP12 antibodies were used to detect endogenous AALP and PEP12 as representatives of soluble and integral membrane proteins, respectively. M, membrane fraction; S, supernatant; T, total protein extracts. (*F*) Quantification of membrane-associated GACP2. The intensity of bands in the immunoblot in *E* was measured using software equipped to LAS4000. For the relative amounts of membrane-associated GAPC2, the band intensity of the M fraction was divided by the combined band intensity of the M and S fractions. (Scale bars: 20 μm.)

McCAP2 was proposed to function as an adaptor for the trafficking of McCPK1. To test this possibility, we examined the subcellular localization of GAPC2. Protoplasts from transgenic plants expressing *AtCAP2:GFP* were immunostained with anti-GAPC2 antibody. GAPC2 colocalized with AtCAP2:GFP at the punctate stains (Fig. 6*C*), indicating that GAPC2 also localizes to the PVC. GAPC1, another cytosolic isoform of GAPDH in *Arabidopsis*, localizes to endomembrane compartments including the TGN, PVC, nucleus, and cytosol (45). These results prompted us to examine whether AtCAP2 plays a role in the localization of GAPC2 to the PVC. GAPC2 localization to the PVC was examined in protoplasts from *atcap2-1* plants by performing immunohistochemistry using an anti-GAPC2 antibody. In contrast to wild-type protoplasts, GAPC2 no longer produced the punctate staining pattern in *atcap2-1* protoplasts, indicating that AtCAP2 plays a role in GAPC2 localization to the PVC (Fig. 6*D*). To confirm this at the biochemical level, protein extracts from wild-type and *atcap2-1* mutant plants were separated by ultracentrifugation, and the soluble and pellet fractions were analyzed by Western blotting using anti-GAPC2 antibody. The pellet fraction of *atcap2-1* extracts contained a significantly reduced amount of GAPC2 compared with that of wild-type extracts; membrane-associated GAPC2 was reduced from 28.15% in wild-type plants to 13.3% in *atcap2-1* plants (Fig. 6*E*). In addition, *gapc2* mutant seedlings also displayed a delay in protein trafficking to the LV (*SI Appendix*, Fig. S10). These results suggest that AtCAP2 is required for the recruitment of GAPC2 to the PVC. These results also support the proposal that AtCAP2 acts together with GAPC2 in vacuolar trafficking.

Discussion

McCAP2, a member of the syntaxin superfamily, was originally proposed to play a role in the plasma membrane-to-nucleus

trafficking of McCPK1, a kinase involved in dehydration stress responses (16). However, we provide compelling evidence that AtCAP2 plays a role in trafficking of proteins to the vacuole. Mutant *atcap2-1* plants display fragmented vacuoles and defects in PSV protein degradation, LV acidification, and LV protein accumulation at early stages of germination, all of which can be explained by defective vacuolar trafficking. Seed germination is a complex process mediated by the conversion of seed embryonic cells to vegetative cells of the growing seedling. The PSV undergoes conversion to the LV during germination, which depends on the correct trafficking and localization of many newly synthesized proteins (3, 18). These proteins include enzymes that degrade PSV proteins, proteins that mediate fusion of PSVs, and proteins that mediate LV acidification and activity. Thus, AtCAP2 contributes to LV biogenesis during germination by supporting the trafficking of certain proteins to PSVs or the newly forming LV. AtCAP2 is specifically involved in vacuolar trafficking because *atcap2-1* plants did not show any defects in secretory and plasma membrane protein trafficking.

An important question is how AtCAP2 is involved in vacuolar trafficking. Although AtCAP2 belongs to the syntaxin superfamily, it does not contain the transmembrane domain or any domains with known functions except for the coiled-coil domain (16). SNAREs also contain coiled-coil domains that interact with components involved in trafficking (42). This suggests that the mechanism of AtCAP2 activity differs from that of SNAREs. AtCAP2 was detected in the soluble fraction and in the membrane-associated fraction. The prominent coiled-coil structure of AtCAP2 raises the possibility that it is an adaptor protein for complexes formed by components of the trafficking machinery. Our co-IP experiments showed that AtCAP2:GFP coprecipitated with GAPC2 (At1g13440), hypothetical protein (At2g13310), and two unknown proteins (At3g07590 and At5g44500). Of the putative interacting proteins, we confirmed that GAPC2, an isoform of GAPDH, interacted with AtCAP2 and colocalized with AtCAP2 at the PVC. Our results showed that AtCAP2 plays a critical role in GAPC2 localization to the PVC, raising the possibility that AtCAP2 plays a role in GAPC2 recruitment to the PVC.

GAPC2 is an isoform of GAPDH, which is involved in sugar metabolism. Recent studies showed that GAPDHs also have other roles, including a role in protein trafficking (37, 39, 41, 46, 47). Plants contain multiple GAPDH isoforms that localize to different subcellular compartments, such as the cytoplasm and chloroplasts. GAPC2, a cytosolic isoform, was identified as a PA-binding protein that plays a critical role in vesicle trafficking (48, 49). GAPC2 is detected in the clathrin-enriched vesicle fraction (38), although the exact role of GAPC2 in protein trafficking has not been determined in plants. In animal cells, GAPDH is involved in vesicle fusion at the ER and Golgi apparatus (37, 50), and provides the energy required for vesicle trafficking along actin filaments (51). In the early secretory pathway in animal cells, Rab2 is thought to recruit GAPDH for vesicle trafficking (47). In plants, GAPC1:GFP associates with vesicles and endomembrane compartments, which led to the proposal that GAPC1 may function in providing the energy that enables vesicular movement (45). In germinating seeds, cells need to reorganize subcellular structures such as the LV. In particular, protein trafficking plays a crucial role in the reorganization (51). In addition, proper supply of resources including energy is also critical for the reorganization (52). We propose that AtCAP2 recruits cytosolic GAPC2 to the PVC, where GAPC2 functions in providing energy to facilitate vacuolar trafficking, which, in turn, contributes to the conversion of PSVs to LVs during germination. AtCAP2 was expressed at higher levels in seeds than in vegetative tissues. However, further investigation is necessary to verify the mechanisms of AtCAP2 and GAPC2 as positive regulators of vacuolar trafficking.

Methods

Plant Materials and Growth Conditions. *Arabidopsis thaliana* plants (ecotype Columbia-0 and *atcap2-1*) were grown on Murashige and Skoog (MS) medium containing 1% sucrose (wt/vol), pH 5.7, in a growth chamber at 20–22 °C under a 16 h light/8 h dark photoperiod.

The T-DNA insertion mutant Salk_209627 (*atcap2-1*) was obtained from the Eurasian *Arabidopsis* Stock Centre at the University of Nottingham (arabidopsis.info). To observe vacuolar morphology or to measure the trafficking efficiency of vacuolar proteins, plants were grown on half-strength MS plates containing 1% sucrose and 0.8% agar at 22°C under a 16 h light/8 h dark photoperiod.

To measure the germination rate, seeds were harvested and stored under the same conditions. Seeds were sterilized and incubated at 4 °C in the dark for 48 h, and then planted on half-strength MS plates containing 1% (wt/vol) sucrose and 0.8% agar. Germination was monitored at 22 °C under a 16 h light/8 h dark photoperiod.

Vacuolar pH Measurement. Vacuolar pH measurements were performed as described previously (20, 51, 53). Cell staining was performed in liquid medium (1/10 MS, 1% sucrose, 10 mM Mes-KOH, pH 5.8) containing 10 μM BCECF-AM in the presence of 0.02% pluronic acid (Invitrogen) for 1 h at 22 °C in the darkness. After staining, seedlings were washed twice for 5 min in 1/10 MS liquid medium. BCECF-AM fluorescence was detected using a laser scanning confocal microscope (LSM510; Carl Zeiss). Images were captured at the root tip and root epidermal cells in germinating seedlings. In situ calibration was performed separately for each root zone. BCECF-AM fluorophore was excited at 488 nm (argon-ion laser) for green or 458 nm (argon-ion laser) for blue, and when monitored with the filter had a spectral detection bandwidth 540 nm. The ratios were obtained using the LSMIB program (software for the LSM510 confocal microscope), and then used to calculate the pH using the calibration curve (*SI Appendix*, Fig. S3 *B* and *C*).

Generation of Transgenic Plants. *AtCAP2* (At2g17990) was isolated by PCR from an *Arabidopsis* cDNA library using the specific primers (*SI Appendix*, Fig. S1). The PCR products were digested with Xba1/Bam H1 and inserted downstream of the cauliflower mosaic virus (CaMV) 35S promoter in a binary vector pCsV1300 (Invitrogen) with CaMV 35S promoter and GFP or RFP. To generate *atcap2-1* plants expressing *AtCAP2:GFP* under the control of its own promoter, we amplified a 1-kb fragment (*AtCAP2p*) of the *AtCAP2* promoter region using specific primers, and used it to substitute the CaMV 35S promoter of pCSV1300. Subsequently, *AtCAP2:GFP* was inserted downstream of *AtCAP2p* to give *AtCAP2p::AtCAP2:GFP*. The construct was introduced into wild-type and *atcap2-1* plants using the *Agrobacterium*-mediated floral dipping method (54). Transgenic plants were screened on B5 plates supplemented with 25 mg/L hygromycin.

To generate mutant plants harboring the vacuolar trafficking marker (AALP:GFP or Spo:GFP) under the Dex-inducible promoter, *atcap2-1* plants were crossed with transgenic plants harboring inducible *AALP:GFP* or *Spo:GFP*. F_1 plants were screened first on B5 plates supplemented with 25 mg/L hygromycin or 30 mg/L kanamycin, and then verified by PCR-mediated genotyping using *atcap2-1*-specific primers. Homozygous plants for both transgenes (*AALP:GFP* or *Spo:GFP*) and the *atcap2-1* mutation were screened at the F_2 generation and confirmed using the phenotypes.

Transient and Stable Expression of Organellar Markers and Vacuolar Cargo Proteins. Plasmids were introduced into protoplasts by polyethylene glycol-mediated transformation (26). Transformed protoplasts were lysed by sonication with lysis buffer [50 mM Tris·HCl, pH 7.5, 150 mM NaCl, 1 mM EDTA, 1 mM EGTA, 0.1% (vol/vol) Triton X-100, and EDTA-free protease inhibitor mixture (Roche)] at 24 or 36 h after transformation. The lysates were centrifuged at 5,000 × *g* for 10 min to eliminate cell debris, and analyzed by immunoblotting with appropriate antibodies.

To induce *AALP:GFP* and *Spo:GFP* expression in transgenic plants, protoplasts were isolated from those transgenic plants at 5 or 12 DAG and treated with 30 μM Dex. Protein extracts were prepared from the protoplasts at appropriate time points after Dex treatment. Cell homogenates were centrifuged, and the cell debris was removed. Protein extracts were analyzed by immunoblotting.

SDS/PAGE and Immunoblot Analysis. Protein samples from protoplasts or plants were separated by SDS/PAGE and analyzed by immunoblotting. After gel electrophoresis, proteins were stained with Coomassie Brilliant Blue R-250, or transferred onto polyvinylidene fluoride (PVDF) membranes. For immunoblot analysis, monoclonal anti-GFP (Clontech), polyclonal anti-AALP,

anti-Actin (MP Biomedicals), anti-α-tubulin (Agrisera), anti-GAPC2 (Agrisera), anti-PIP2;1 (Agrisera), anti-T7 (Novagen), and anti-TIP1;1 (Agrisera) antibodies were used. Protein blots were developed using Western blot detection solution (Supex) and visualized using the LAS4000 imaging system (FUJIFILM). The protein band intensities were quantified with dedicated software for the LAS4000.

In Vivo Localization of AtCAP2 in *Arabidopsis* Protoplasts. To investigate the subcellular localization of AtCAP2, protoplasts were isolated from transgenic plants expressing *AtCAP2:GFP*, and transformed with organellar markers by PEG-mediated transformation. Images were acquired with a fluorescence microscope (Carl Zeiss AxioPlan2) or a laser scanning confocal microscope (LSM510; Carl Zeiss) (26). Images were processed using Adobe Photoshop. To analyze signal colocalization, Pearson's coefficients were obtained using ImageJ 1.50a (National Institutes of Health).

Subcellular Fractionation Analysis. Protoplasts were isolated from transgenic plants expressing *AtCAP2:GFP* and suspended in sonication buffer (20 mM Tris·HCl, 2.5 mM $MgCl_2$, 2 mM EGTA, 1 mM EDTA, and 150 mM NaCl). Protoplasts were disrupted by sonication. After centrifugation, cell debris was discarded and the soluble fraction was subjected to ultracentrifugation at 100,000 × *g* for 90 min. Proteins from the soluble and pellet fractions were collected separately and analyzed by immunoblotting using anti-GFP antibody. AALP and PEP12 were detected as fractionation controls using anti-AALP and anti-PEP12 antibodies, respectively.

For alkali treatment, microsomal pellets were resuspended in 130 μL of alkaline buffer (0.1 M Na_2CO_3, pH 11.1, 0.3 M sucrose, 5 mM EGTA, and 5 mM $MgCl_2$). The suspension was incubated for 10 min on ice and then subjected to ultracentrifugation at 100,000 × *g* for 30 min at 4 °C to separate the supernatant and pellet fractions. These fractions were analyzed by Western blotting.

Immunoprecipitation and Mass Spectrometry. Total cell lysates from 5-d-old seedlings were prepared in IP buffer (10 mM Tris·HCl, pH 7.4, 150 mM NaCl, 0.5 mM EDTA, 0.2% Nonidet P-40, 5% glycerol, and 1 × cOmplete protease inhibitor mixture) and incubated with GFP-Trap agarose beads (ChromoTek) in a top-to-end rotator at 4 °C for 4 h. After incubation, the beads were washed 10 times with ice-cold washing buffer (10 mM Tris·HCl, pH 7.4, 150 mM NaCl, 0.5 mM EDTA, and 0.1% Nonidet P-40) and then eluted by boiling in reducing SDS sample buffer. Proteins were separated by SDS/PAGE and subjected to MS analysis.

Sample preparation for MS was performed as described previously (55, 56). Briefly, the gel was silver-stained after SDS/PAGE separation, and the protein bands were cut out for in-gel trypsin digestion overnight at 30 °C. The digested peptide mixture was loaded on a PepMap100 C18 nano column using the Nano-LC System (Bruker). Collected samples were further analyzed using a MALDI/TOF/TOF analyzer (Ultraflextreme; Bruker). Mass data acquisitions were piloted by FlexControl software using automatic run. MS and MS/MS data were loaded into Proteinscape software 3.0 (Bruker) and searched against the National Center for Biotechnology Information nonredundant database with species restriction to *Arabidopsis* by Mascot search engine (Matrix Sciences). Only significant hits, which are defined by Mascot probability analysis and with at least one matched peptide, were accepted.

ACKNOWLEDGMENTS. This work was carried out with the support of "Cooperative Research Program for Agriculture Science and Technology Development (Project PJ010953012018)" Rural Development Administration, Republic of Korea.

1. Frigerio L, Hinz G, Robinson DG (2008) Multiple vacuoles in plant cells: Rule or exception? *Traffic* 9:1564–1570.
2. Feeney M, Frigerio L, Kohalmi SE, Cui Y, Menassa R (2013) Reprogramming cells to study vacuolar development. *Front Plant Sci* 4:493.
3. Zheng H, Staehelin LA (2011) Protein storage vacuoles are transformed into lytic vacuoles in root meristematic cells of germinating seedlings by multiple, cell type-specific mechanisms. *Plant Physiol* 155:2023–2035.
4. Banta LM, Robinson JS, Klionsky DJ, Emr SD (1988) Organelle assembly in yeast: Characterization of yeast mutants defective in vacuolar biogenesis and protein sorting. *J Cell Biol* 107:1369–1383.
5. Raymond CK, Roberts CJ, Moore KE, Howald I, Stevens TH (1992) Biogenesis of the vacuole in Saccharomyces cerevisiae. *Int Rev Cytol* 139:59–120.
6. Wada Y, Anraku Y (1992) Genes for directing vacuolar morphogenesis in Saccharomyces cerevisiae. II. VAM7, a gene for regulating morphogenic assembly of the vacuoles. *J Biol Chem* 267:18671–18675.
7. Rojo E, Zouhar J, Kovaleva V, Hong S, Raikhel NV (2003) The AtC-VPS protein complex is localized to the tonoplast and the prevacuolar compartment in arabidopsis. *Mol Biol Cell* 14:361–369.
8. Rojo E, Gillmor CS, Kovaleva V, Somerville CR, Raikhel NV (2001) VACUOLELESS1 is an essential gene required for vacuole formation and morphogenesis in Arabidopsis. *Dev Cell* 1:303–310.
9. Feraru E, et al. (2010) The AP-3 β adaptin mediates the biogenesis and function of lytic vacuoles in Arabidopsis. *Plant Cell* 22:2812–2824.
10. Isono E, et al. (2010) The deubiquitinating enzyme AMSH3 is required for intracellular trafficking and vacuole biogenesis in Arabidopsis thaliana. *Plant Cell* 22:1826–1837.
11. Kolb C, et al. (2015) FYVE1 is essential for vacuole biogenesis and intracellular trafficking in Arabidopsis. *Plant Physiol* 167:1361–1373.
12. Laval V, et al. (2003) Seed germination is blocked in Arabidopsis putative vacuolar sorting receptor (atbp80) antisense transformants. *J Exp Bot* 54:213–221.
13. Shimada T, et al. (2003) Vacuolar sorting receptor for seed storage proteins in Arabidopsis thaliana. *Proc Natl Acad Sci USA* 100:16095–16100.
14. Lee Y, et al. (2013) Functional identification of sorting receptors involved in trafficking of soluble lytic vacuolar proteins in vegetative cells of Arabidopsis. *Plant Physiol* 161:121–133.
15. Zwiewka M, et al. (2011) The AP-3 adaptor complex is required for vacuolar function in Arabidopsis. *Cell Res* 21:1711–1722.
16. Chehab EW, Patharkar OR, Cushman JC (2007) Isolation and characterization of a novel v-SNARE family protein that interacts with a calcium-dependent protein kinase from the common ice plant, Mesembryanthemum crystallinum. *Planta* 225:783–799.
17. Martinière A, et al. (2013) In vivo intracellular pH measurements in tobacco and Arabidopsis reveal an unexpected pH gradient in the endomembrane system. *Plant Cell* 25:4028–4043.
18. Wilson KA, Chavda BJ, Pierre-Louis G, Quinn A, Tan-Wilson A (2016) Role of vacuolar membrane proton pumps in the acidification of protein storage vacuoles following germination. *Plant Physiol Biochem* 104:242–249.
19. Brauer D, Otto J, Tu S-I (1995) Selective accumulation of fluorescent pH indicator, BCECF, in vacuoles of maize root-hair cells. *J Plant Physiol* 145:57–61.
20. Krebs M, et al. (2010) Arabidopsis V-ATPase activity at the tonoplast is required for efficient nutrient storage but not for sodium accumulation. *Proc Natl Acad Sci USA* 107:3251–3256.
21. Nishimura M (1982) pH in vacuoles isolated from castor bean endosperm. *Plant Physiol* 70:742–744.
22. He F, Huang F, Wilson KA, Tan-Wilson A (2007) Protein storage vacuole acidification as a control of storage protein mobilization in soybeans. *J Exp Bot* 58:1059–1070.
23. Ozkan P, Mutharasan R (2002) A rapid method for measuring intracellular pH using BCECF-AM. *Biochim Biophys Acta* 1572:143–148.
24. Klemens PA, et al. (2013) Overexpression of the vacuolar sugar carrier AtSWEET16 modifies germination, growth, and stress tolerance in Arabidopsis. *Plant Physiol* 163:1338–1352.
25. Sohn EJ, et al. (2003) Rha1, an Arabidopsis Rab5 homolog, plays a critical role in the vacuolar trafficking of soluble cargo proteins. *Plant Cell* 15:1057–1070.
26. Kang H, et al. (2012) Trafficking of vacuolar proteins: The crucial role of Arabidopsis vacuolar protein sorting 29 in recycling vacuolar sorting receptor. *Plant Cell* 24:5058–5073.
27. Jung C, et al. (2011) Identification of sorting motifs of AtβFruct4 for trafficking from the ER to the vacuole through the Golgi and PVC. *Traffic* 12:1774–1792.
28. Maurel C, Santoni V, Luu D-T, Wudick MM, Verdoucq L (2009) The cellular dynamics of plant aquaporin expression and functions. *Curr Opin Plant Biol* 12:690–698.
29. Kim H, Park M, Kim SJ, Hwang I (2005) Actin filaments play a critical role in vacuolar trafficking at the Golgi complex in plant cells. *Plant Cell* 17:888–902.
30. Wu X, Ebine K, Ueda T, Qiu Q-S (2016) AtNHX5 and AtNHX6 are required for the subcellular localization of the SNARE complex that mediates the trafficking of seed storage proteins in Arabidopsis. *PLoS One* 11:e0151658.
31. Sanderfoot AA, Kovaleva V, Bassham DC, Raikhel NV (2001) Interactions between syntaxins identify at least five SNARE complexes within the Golgi/prevacuolar system of the Arabidopsis cell. *Mol Biol Cell* 12:3733–3743.
32. Jaillais Y, Fobis-Loisy I, Miège C, Rollin C, Gaude T (2006) AtSNX1 defines an endosome for auxin-carrier trafficking in Arabidopsis. *Nature* 443:106–109.
33. De Benedictis M, et al. (2013) AtSYP51/52 functions diverge in the post-Golgi traffic and differently affect vacuolar sorting. *Mol Plant* 6:916–930.
34. Nielsen E, Cheung AY, Ueda T (2008) The regulatory RAB and ARF GTPases for vesicular trafficking. *Plant Physiol* 147:1516–1526.
35. Song J, Lee MH, Lee GJ, Yoo CM, Hwang I (2006) Arabidopsis EPSIN1 plays an important role in vacuolar trafficking of soluble cargo proteins in plant cells via interactions with clathrin, AP-1, VTI11, and VSR1. *Plant Cell* 18:2258–2274.
36. Robbins AR, Ward RD, Oliver C (1995) A mutation in glyceraldehyde 3-phosphate dehydrogenase alters endocytosis in CHO cells. *J Cell Biol* 130:1093–1104.
37. Tisdale EJ, Kelly C, Artalejo CR (2004) Glyceraldehyde-3-phosphate dehydrogenase interacts with Rab2 and plays an essential role in endoplasmic reticulum to Golgi transport exclusive of its glycolytic activity. *J Biol Chem* 279:54046–54052.
38. McLoughlin F, et al. (2013) Identification of novel candidate phosphatidic acid-binding proteins involved in the salt-stress response of Arabidopsis thaliana roots. *Biochem J* 450:573–581.
39. Tisdale EJ, Talati NK, Artalejo CR, Shisheva A (2016) GAPDH binds Akt to facilitate cargo transport in the early secretory pathway. *Exp Cell Res* 349:310–319.
40. Kaneda M, Takeuchi K, Inoue K, Umeda M (1997) Localization of the phosphatidylserine-binding site of glyceraldehyde-3-phosphate dehydrogenase responsible for membrane fusion. *J Biochem* 122:1233–1240.
41. Glaser PE, Han X, Gross RW (2002) Tubulin is the endogenous inhibitor of the glyceraldehyde 3-phosphate dehydrogenase isoform that catalyzes membrane fusion:

Implications for the coordinated regulation of glycolysis and membrane fusion. *Proc Natl Acad Sci USA* 99:14104–14109.
42. Nakagawa T, et al. (2003) Participation of a fusogenic protein, glyceraldehyde-3-phosphate dehydrogenase, in nuclear membrane assembly. *J Biol Chem* 278: 20395–20404.
43. Guo L, et al. (2012) Cytosolic glyceraldehyde-3-phosphate dehydrogenases interact with phospholipase Dδ to transduce hydrogen peroxide signals in the Arabidopsis response to stress. *Plant Cell* 24:2200–2212.
44. Testerink C, Munnik T (2005) Phosphatidic acid: A multifunctional stress signaling lipid in plants. *Trends Plant Sci* 10:368–375.
45. Henry E, Fung N, Liu J, Drakakaki G, Coaker G (2015) Beyond glycolysis: GAPDHs are multi-functional enzymes involved in regulation of ROS, autophagy, and plant immune responses. *PLoS Genet* 11:e1005199.
46. Tisdale EJ (2001) Glyceraldehyde-3-phosphate dehydrogenase is required for vesicular transport in the early secretory pathway. *J Biol Chem* 276:2480–2486.
47. König S, Ischebeck T, Lerche J, Stenzel I, Heilmann I (2008) Salt-stress-induced association of phosphatidylinositol 4,5-bisphosphate with clathrin-coated vesicles in plants. *Biochem J* 415:387–399.
48. Jiang Y, et al. (2016) Phosphatidic acid produced by RalA-activated PLD2 stimulates caveolae-mediated endocytosis and trafficking in endothelial cells. *J Biol Chem* 291: 20729–20738.
49. Bryksin AV, Laktionov PP (2008) Role of glyceraldehyde-3-phosphate dehydrogenase in vesicular transport from golgi apparatus to endoplasmic reticulum. *Biochemistry (Mosc)* 73:619–625.
50. Hinckelmann MV, et al. (2016) Self-propelling vesicles define glycolysis as the minimal energy machinery for neuronal transport. *Nat Commun* 7:13233.
51. Viotti C, et al. (2013) The endoplasmic reticulum is the main membrane source for biogenesis of the lytic vacuole in Arabidopsis. *Plant Cell* 25:3434–3449.
52. Stefano G, Renna L, Moss T, McNew JA, Brandizzi F (2012) In Arabidopsis, the spatial and dynamic organization of the endoplasmic reticulum and Golgi apparatus is influenced by the integrity of the C-terminal domain of RHD3, a non-essential GTPase. *Plant J* 69:957–966.
53. Kriegel A, et al. (2015) Job sharing in the endomembrane system: Vacuolar acidification requires the combined activity of V-ATPase and V-PPase. *Plant Cell* 27: 3383–3396.
54. Clough SJ, Bent AF (1998) Floral dip: A simplified method for Agrobacterium-mediated transformation of Arabidopsis thaliana. *Plant J* 16:735–743.
55. Gao C, et al. (2012) The Golgi-localized Arabidopsis endomembrane protein12 contains both endoplasmic reticulum export and Golgi retention signals at its C terminus. *Plant Cell* 24:2086–2104.
56. Shen J, et al. (2013) An in vivo expression system for the identification of cargo proteins of vacuolar sorting receptors in Arabidopsis culture cells. *Plant J* 75: 1003–1017.